

## Size-dependent optical and electrochemical band gaps of ZnS nanorods fabricated through single molecule precursor route

B. Y. Geng,<sup>a)</sup> X. W. Liu, J. Z. Ma, and Q. B. Du

Anhui Key Laboratory of Functional Molecular Solids, College of Chemistry and Materials Science, Anhui Normal University, Wuhu 241000, People's Republic of China

L. D. Zhang

Institute of Solid State Physics, Chinese Academy of Sciences, Hefei 230031, People's Republic of China

(Received 6 February 2007; accepted 3 April 2007; published online 1 May 2007)

The colloidal, highly crystalline, and size-controlled ZnS nanorods have been prepared through a thermal decomposition of single-source-precursor approach in oleylamine solution. The length and width of nanorods can be controlled simply by varying the molar ratio of zinc 2-mercaptobenzothiazole complex and oleylamine or prolonging the anneal duration. Optical and electrochemical properties of different sizes of ZnS nanorods are discussed and size-dependent optical and electrochemical band gaps are evidently observed, which show a direct correlation between the electronic spectra and electrochemical band gap. © 2007 American Institute of Physics. [DOI: 10.1063/1.2734385]

Recently, one-dimensional (1D) nanocrystalline materials, including nanorods and nanowires, have been intensively investigated for their unique properties, which are derived from their low dimensionality.<sup>1,2</sup> As one of the most important group II-VI semiconductors, ZnS with a band gap of 3.66 eV at room temperature is a traditional phosphor, which was widely used in flat-panel display, electroluminescent devices, infrared windows, sensors, and lasers.<sup>3,4</sup> Several different synthetic methods have been used to synthesize 1D ZnS nanostructures.<sup>5-11</sup> However, the synthesis of high quality ZnS nanostructures with uniform size, shape, and good optical properties is still a challenge. Nanocrystals, synthesized using a wet chemistry technique, can grow continually in the solution by coarsening or epitaxial attachment due to the scarcity of a strong repelling organic layer on the particle surface and lead to aggregation or precipitation over a few days.<sup>12</sup> In this letter, we report the preparation of colloidal, highly crystalline, and size-controlled ZnS nanorods through a thermal decomposition of single-source-precursor approach in oleylamine (OA) solution with a similar process reported by Zhang *et al.*,<sup>13</sup> as well as their size-dependent optical and electrochemical properties. In this case, zinc 2-mercaptobenzothiazole complex [Zn(Mer)<sub>2</sub>] was used as single-source precursor to fabricate ZnS nanorods. Zn(Mer)<sub>2</sub> is air stable and synthesizes easily using a similar process reported by Rockenberger *et al.*<sup>14</sup> The length and width of nanorods can be controlled simply by varying the molar ratio of Zn(Mer)<sub>2</sub> and OA or prolonging the anneal duration. Moreover, we study the electrochemical properties of ZnS nanorods and demonstrate a direct correlation between their electrochemical band gap and the electronic spectra in CH<sub>2</sub>Cl<sub>2</sub>, as the electrochemical properties of semiconductors are investigated poorly because the limited solvent window of many solvent/electrolyte systems, the instability and the insolubility of nanocrystals.

The synthetic procedure of Zn(Mer)<sub>2</sub> can be simply describe as follows: 0.02 mol 2-mercaptobenzothiazole was dissolved in 20 ml ethanol, and 0.01 mol Zn (CH<sub>3</sub>COO)<sub>2</sub>

was also dissolved in 10 ml ethanol. The above two solutions were mixed together under stirring; the mixture was put into an ice-water bath for 30 min and filtered. The precipitate was collected, washed with de-ionized water, and dried *in vacuo* at 60 °C overnight.

The ZnS nanorods were fabricated from the precursor Zn(Mer)<sub>2</sub> obtained from the above experiment. For sample 1, 8 ml OA was added in a three-necked flask at room temperature, and then the solvent was removed under vacuum at about 100 °C for 30 min. After the solvent was cooled to room temperature, 0.58 mmol Zn(Mer)<sub>2</sub> was added to the flask, and then Ar was bubbled through the solution for 20 min. The flask was then flash heated to 270 °C and aged for 7 h in inert atmosphere. After centrifugation, pale white powder was obtained. The pale white powder was washed with ethanol several times in order to remove excess OA in the products and dried *in vacuo* for further characterization. Sample 2 was synthesized under similar synthetic conditions with an anneal duration of 3.5 h, while sample 3 was synthesized using 15 ml OA with an anneal duration of 7 h.

The synthesized products were characterized by x-ray diffraction (XRD) (MAC Science MXP 18AHF), selected-area electron diffraction (SAED) and transmission electron microscopy (TEM) (JEM 200CX), high-resolution TEM (HRTEM) (JEOL 2010), room temperature UV/visible absorption [U-3010 UV/visible spectrophotometer (220 V, 50 Hz)], and photoluminescence (PL) (F-4500) using 250 nm as the excitation wavelength with a Xe arc lamp at room temperature. The electrochemical properties of the nanorods were investigated by cyclic voltammetry (CV) at a Au electrode with tetra-*n*-butylammonium perchlorate (TBAP) as supporting electrolyte in freshly distilled CH<sub>2</sub>Cl<sub>2</sub>. A three-electrode configuration was used where Pt coil and Ag/AgCl electrode served as the counter and reference electrodes, respectively.

The TEM images (Fig. 1) reveal that the sizes of the nanorods can be controlled simply by varying the molar ratio of Zn(Mer)<sub>2</sub> and OA or prolonging the anneal duration. The HRTEM images of the nanorods indicate the highly crystalline nature of these nanorods. They also reveal that the interplanar distances along the growth axis are 0.311 nm, which

<sup>a)</sup> Author to whom correspondence should be addressed: FAX: +86-553-3869303; Electronic mail: bygeng@mail.ahnu.edu.cn

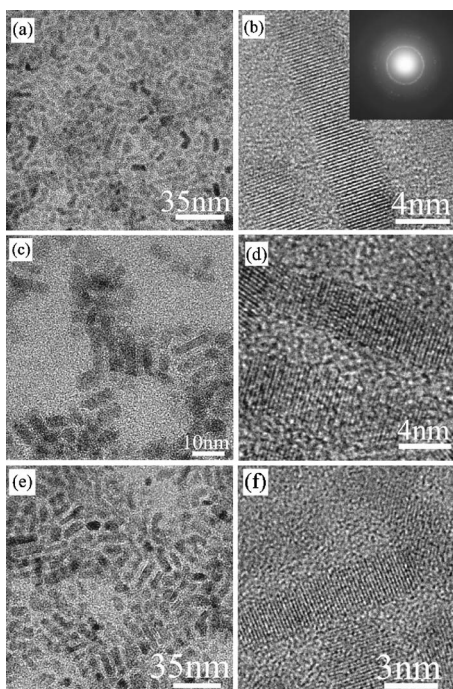


FIG. 1. TEM and HRTEM images of ZnS nanorods. Reaction conditions: 7 h, 8 ml OA for (a) and (b); 3.5 h, 8 ml OA for (c) and (d); and 7 h, 15 ml OA for (e) and (f). The inset in (b) is the SAED pattern of sample 1.

is consistent with the interplanar distance of the (110) plane of the hexagonal wurtzite structure of ZnS. The SAED pattern [inset in Fig. 1(b)] can be indexed to the hexagonal structure, which is consistent with the corresponding XRD data. When 8 ml OA was used and aged for 7 h at 270 °C, the obtained nanorods had average size of about 5 nm (diameter)  $\times$  24 nm (length). If the reaction was kept at 270 °C for 3.5 h, the shorter nanorods with length lower than 12 nm were obtained [Figs. 1(c) and 1(d)]. It is important to note that some preformed nanorods, which contained a few primary particles, have been observed, which may demonstrate that the nanorod formation may base on the oriented attachment mechanism.<sup>15</sup> If 15 ml OA was used, the products are shown in Figs. 1(e) and 1(f). The nanorods have a smaller size with a diameter of about 3 nm and 17 nm in length, indicating that the concentration of OA plays an important role in rod-growth process. Furthermore, by changing the synthetic conditions, the sizes of ZnS nanorods can be controlled accurately, which are shown in Table I.

The typical XRD patterns of the as-synthesized products are shown in Fig. 2, and all of the detectable diffraction peaks are indexed to those from hexagonal ZnS,<sup>16</sup> revealing the pure sample phase. All XRD patterns show obvious size-broadening effects, indicating the finite size of these nano-

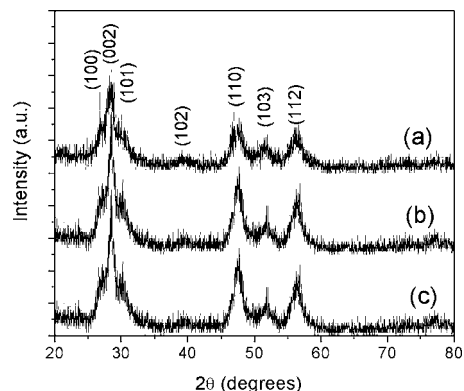


FIG. 2. XRD patterns taken from as-synthesized products. (a) 3.5 h, 8 ml OA; (b) 7 h, 15 ml OA; and (c) 7 h, 8 ml OA.

crystals, which is a general size-dependent phenomenon in nanoparticles. Compared to samples 1 and 3, peaks of sample 2 are not very obvious for a shorter anneal duration.

Figures 3(a) and 3(b) show the UV/visible absorption and room temperature PL (excitation at 250 nm) spectra of the as-prepared ZnS nanorods. The absorption peaks are located around 310 nm for sample 1, 300 nm for sample 2, and 305 nm for sample 3, which clearly exhibit blueshifted about 30, 40, and 35 nm, respectively, compared to the bulk band-gap wavelength (340 nm), which may be caused by excitonic transition. The long absorption tail of all samples was due to scattering by the crystal. Figure 3(b) illustrates the room temperature PL of as-prepared ZnS nanorods with different sizes. The emission maximum appears at 364 nm (3.41 eV) for sample 1, 354 nm (3.51 eV) for sample 2, and 360 nm

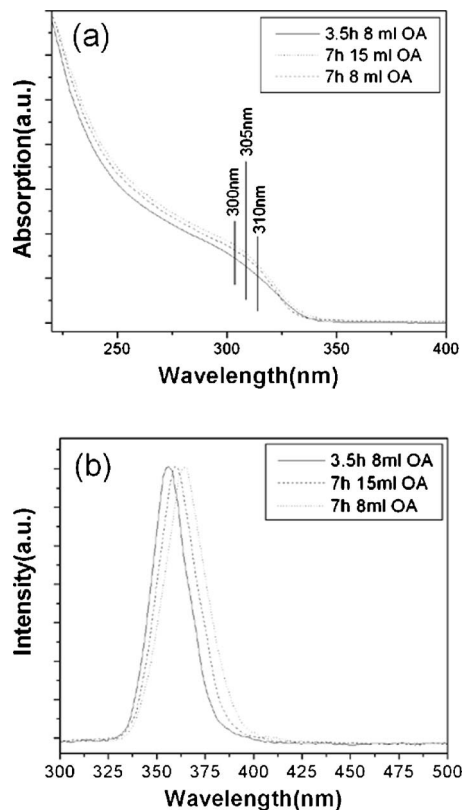


FIG. 3. (a) UV-visible spectra of the as-prepared ZnS nanorods dispersed in cyclohexane. (b) Photoluminescence spectra of as-prepared ZnS nanorods dispersed in cyclohexane.

TABLE I. Sizes of the as-prepared ZnS nanorods under different conditions.

No.	Zn (Mer) <sub>2</sub> (mmol)	OA (mL)	T (°C)	t (h)	Size (diameter $\times$ length) (nm <sup>2</sup> )
1	0.58	8	270	7	5 $\times$ 24
2	0.58	8	270	3.5	5 $\times$ 11
3	0.58	8	270	12	5.5 $\times$ 32
4	0.58	15	270	7	3 $\times$ 17
5	0.58	22	270	7	2 $\times$ 14
6	0.58	15	270	12	3 $\times$ 25

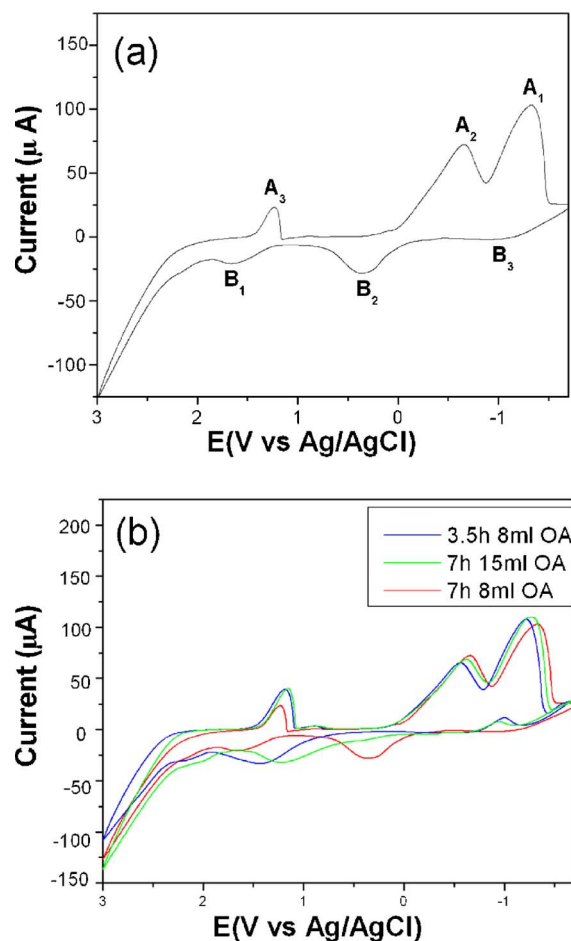


FIG. 4. (Color online) (a) CV response in presence of OA-capped ZnS nanorod (1 mg/ml of sample 1) at a Au electrode. Sweep rate=100 mV/s and [TBAP]=0.05 M. (b) CVs illustrating the electrochemical band gap ( $A_1$ – $B_1$  peak separation) for all samples. [ZnS nanorod]=1 mg/ml, [TBAP]=0.05 M, and sweep rate=100 mV/s.

(3.45 eV) for sample 3, indicating that the band gap of the three kinds of ZnS nanorods is changed slightly with variation of the size.

Figure 4(a) shows a typical CV for sample 1 at the Au electrode. It is noteworthy that ZnS nanorods with different sizes synthesized in this letter have good solubility in  $\text{CH}_2\text{Cl}_2$ , which is different from the thioglycerol-capped CdS nanoparticles which have size-dependent solubility.<sup>17</sup> The peak currents increased as the concentration of ZnS nanorods was enhanced and the peak potential without notable change. From the CV, several prominent oxidation and reduction peaks are located between  $-1.42$  V ( $A_1$ ) and  $1.74$  V ( $B_2$ ); furthermore,  $A_2$ ,  $A_3$  and  $B_2$ ,  $B_3$  appeared only after scan reversal passing  $B_1$  and  $A_1$ , which confirmed that  $B_1$  reduction products were reoxidized at  $A_2$  and  $A_3$  and  $A_1$  oxidation products were reduced at  $B_2$  and  $B_3$ . These might correspond to ZnS/Zn and ZnS/S couples. The peak-to-peak separation between  $A_1$  and  $B_1$  is 3.12 V and is a useful correlation of electron spectra because the separation is caused by the transition of electrons between highest occupied molecular orbital (HOMO) and lowest unoccupied molecular orbital (LUMO). Chen *et al.* have observed a similar correlation between the optical and the electrochemical gap from alkanethiol-capped gold nanoparticles.<sup>18</sup> In the case of Au

nanoparticles, electron transfer to the particle cannot cause a reduction reaction for the stability of thiol-capped gold nanoparticles and charging the particle double-layer discretely results in electrochemical analogs of Coulomb staircase charging. However, transition metal sulfide nanoparticles are not as stable as Au nanoparticles, and electron transfer process can cause a series of chemical reactions.<sup>19</sup>

Figure 4(b) illustrates the CVs of different samples, from which the different peak-to-peak separations are obviously observed. The shapes of all CVs are similar, and the current potentials are shifted slightly as the sizes are varied. The peak-to-peak separation of sample 1 is about 3.18 V, 3.38 V for sample 2, and 3.26 V for sample 3, indicating that the gap between HOMO and LUMO is size dependent, which is perfectly consistent with the optical band gap.

In summary, ZnS nanorods with different sizes have been synthesized through a single-source-precursor approach by controlling the molar ratio of  $\text{Zn}(\text{Mer})_2$  and OA or the reaction duration. Optical and electrochemical properties of different sizes of ZnS nanorods are discussed and size-dependent optical and electrochemical band gaps are evidently observed, which show a direct correlation between the electronic spectra and electrochemical band gap.

This work was supported by the National Natural Science Foundation of China (20671003), the Foundation of Key Project of Natural Science of Anhui Education Committee (2006kj041a), the Young Teacher Sustainment Project of Anhui (Grant No. 2005jq1041zd), and the Education Department of Anhui Province (2006KJ006TD).

- <sup>1</sup>J. Hu, L. S. Li, W. Yang, L. Manna, L. W. Wang, and A. P. Alivisatos, *Science* **292**, 2060 (2001).
- <sup>2</sup>J. Park, B. Koo, Y. Hwang, C. Bae, K. An, J.-G. Park, H. M. Park, and T. Hyeon, *Angew. Chem., Int. Ed.* **43**, 2282 (2004).
- <sup>3</sup>E. Monroy, F. Omnes, and F. Calle, *Semicond. Sci. Technol.* **18**, R33 (2003).
- <sup>4</sup>W. Park, J. S. King, C. W. Neff, C. Liddell, and C. Summers, *Phys. Status Solidi B* **229**, 949 (2002).
- <sup>5</sup>Q. Li and C. R. Wang, *Appl. Phys. Lett.* **83**, 359 (2003).
- <sup>6</sup>Y. Jiang, X. M. Meng, J. Liu, Z. Y. Xie, C. S. Lee, and S. T. Lee, *Adv. Mater. (Weinheim, Ger.)* **15**, 323 (2003).
- <sup>7</sup>S. H. Yu and M. Yoshimura, *Adv. Mater. (Weinheim, Ger.)* **14**, 296 (2002).
- <sup>8</sup>X. C. Jiang, Y. Xie, J. Lu, L. Y. Zhu, W. He, and Y. T. Qian, *Chem. Mater.* **13**, 1213 (2001).
- <sup>9</sup>Y. Jiang, X. M. Meng, J. Liu, Z. R. Hong, C. S. Lee, and S. T. Lee, *Adv. Mater. (Weinheim, Ger.)* **15**, 1195 (2003).
- <sup>10</sup>X. Wang, J. Zhuang, Q. Peng, and Y. Li, *Nature (London)* **437**, 121 (2005).
- <sup>11</sup>Y. Li, X. Li, C. Yang, and Y. Li, *J. Phys. Chem. B* **108**, 16002 (2004).
- <sup>12</sup>P. D. Cozzoli, A. Kornowski, and H. Weller, *J. Phys. Chem. B* **109**, 2638 (2005).
- <sup>13</sup>Y. C. Zhang, G. Y. Wang, X. Y. Hu, and W. W. Chen, *Mater. Res. Bull.* **41**, 1817 (2006).
- <sup>14</sup>J. Rockenberger, E. C. Scher, and A. P. Alivisatos, *J. Am. Chem. Soc.* **121**, 11595 (1999).
- <sup>15</sup>J. H. Yu, J. Joo, H. M. Park, S. Baik, Y. W. Kim, S. C. Kim, and T. Hyeon, *J. Am. Chem. Soc.* **127**, 5662 (2005).
- <sup>16</sup>JCPDS-International Center for Diffraction Data No. 80-0007.
- <sup>17</sup>S. K. Haram, B. M. Quinn, and A. J. Bard, *J. Am. Chem. Soc.* **123**, 8860 (2001).
- <sup>18</sup>S. Chen, R. S. Ingrma, M. J. Hostwtler, J. J. Pietron, R. W. Murray, T. G. Schaaff, J. T. Khoury, M. M. Alvarez, and R. L. Whetten, *Science* **280**, 2098 (1998).
- <sup>19</sup>S. Chen, L. A. Truax, and J. M. Sommers, *Chem. Mater.* **12**, 3864 (2000).